ELSEVIER

Chemical Engineering Journal 140 (2008) 621–625

Chemical Engineering Journal

www.elsevier.com/locate/cej

Short communication

Study of TiC/Ni_3Al composites by laser ignited self-propagating high-temperature synthesis (LISHS)

Y.X. Li, J.D. Hu, H.Y. Wang, Z.X. Guo*

Jilin University, College of Materials Science and Engineering, The Key Lab of Automobile Materials, Ministry of Education,
Renmin Street No. 5988, Changchun 130025, PR China

Received 11 September 2007; received in revised form 11 November 2007; accepted 26 November 2007

Abstract

TiC/Ni_3Al composites have been obtained in situ by laser ignited self-propagating high-temperature synthesis (LISHS) of an intimate mixture of compacted powders of elemental C, Ti, Ni and Al. Ignition temperature (T_{ig}) and combustion temperature (T_c) are investigated; the effects of Ni_3Al content on density, phase composition, microstructure of the reaction products and particle size of the synthesized TiC were studied. The results show the density of the products varies with Ni_3Al content, and a maximum value of density appears at 50 wt.% Ni_3Al; TiC and Ni_3Al are the two stable phases after SHS, TiC particle size decreases with the increasing of Ni_3Al content, however, the decreasing of grain size is unobvious when Ni_3Al content is over 60 wt.%.

Keywords: Composite materials; Laser ignited self-propagating high-temperature synthesis (LISHS); Thermodynamic properties; Microstructure

1. Introduction

Self-propagating high-temperature synthesis (SHS) of inorganic compounds has a number of essential advantages over comparable methods of intermetallic synthesis. These advantages include:

- Low power input.
- Self-cleaning of the synthesized product (resulting from combustion).
- SHS results directly in the creation of a powder [1–4].

The method is based on the use of the heat released during exothermic reactions in order to preheat raw materials and to obtain a self-sustained system. Reaction is started by the use of a laser and after ignition the reactions proceed as a reaction front with linear speeds of 1–100 mm/s through the compacted raw materials in powder form. Temperature in the reaction front is related to the reaction synthesis, compaction of the raw materials, specific surface and other processing parameters [7] and reach up to a few thousands of degrees. The procedure has a low energy consumption due to the high productivity and the very simple equipment involved. Hereafter we refer this process as laser igniting self-propagating high-temperature synthesis (LISHS). Fig. 1 shows schematics of the combustion synthesis using the SHS process.

Ni_3Al phase is an intermetallic with excellent corrosion and oxidation resistance in a wide range of temperatures owing to formation of a stable surface alumina oxide layer and strongly stable chemical and phase stabilities up to high temperatures close to their melting points [5–8], and TiC is a ceramic with high melting point, extreme hardness, low density, moderate fracture toughness, and high resistance to oxidation and corrosion [9–11] and a very good wettability with Ni_3Al [12]. Therefore, considerable effort has been made to investigate the combustion synthesis of TiC/Ni_3Al. Mei et al. [13] investigated the mechanism of combustion synthesis of Ti–C–3Ni–Al system; Keskinen et al. [14] studied the mechanical and high-temperature properties of TiC/Ni_3Al; Zhang et al. [15] investigated the cyclic thermal shock characteristics of TiC/Ni_3Al FGMs, and so on. Clearly, the above-mentioned results are based on the observation of mechanism of combustion synthesis and of its products. Therefore, it is necessary to study more carefully the effect of composition on products synthesized.

---

* Corresponding author. Tel.: +86 431 85095326; fax: +86 431 85095876.
E-mail address: ldb@jlu.edu.cn (Z.X. Guo).

1385-8947/$ – see front matter © 2007 Elsevier B.V. All rights reserved.
doi:10.1016/j.cej.2007.11.034

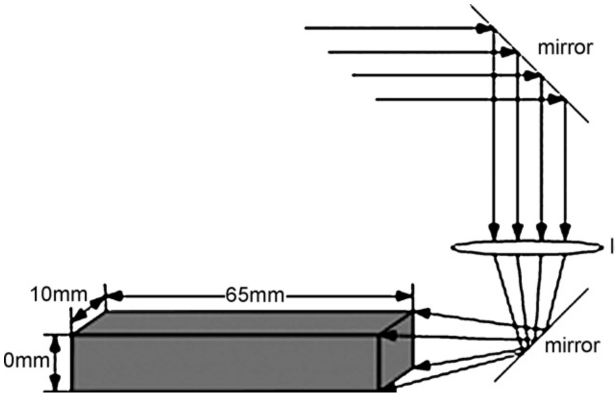

Fig. 1. Scheme of combustion synthesis by the LISHS process.

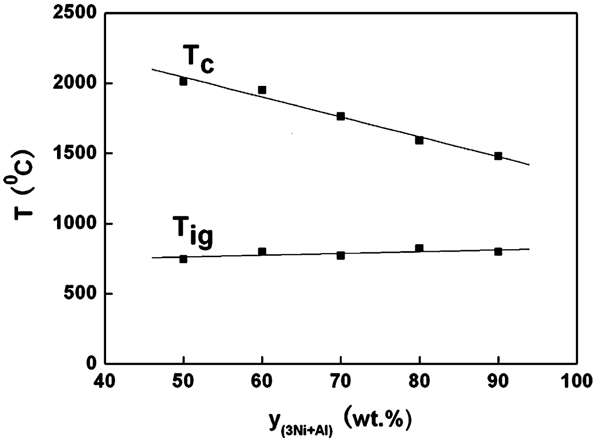

Fig. 2. Effect of y-value on T_{ig} and T_c of Ti–C–3Ni–Al system.

The aim of our work has been to prove the feasibility of obtaining TiC/Ni_3Al intermetallic cermets by LISHS and investigate the effect of Ni_3Al content on microstructure and phase composition of Ti–C–3Ni–Al reacting product so that the laws of structure formation of the products should be understood, which should provide guidance for the alteration and control of the structure of the product phases.

2. Experimental procedures

The powders of Ni, Al, Ti and C (graphite) with a nominal purity of 99.9, 98.6, 98.0 and 99.9%, respectively, and average particle sizes of 30–60 μm in metals and 38 μm in carbon, were used for the preparation of the Ti–C–3Ni–Al mixtures. Reagent powder mixtures were prepared for the following the basic reaction:

$$(\mathrm{Ti} + \mathrm{C}) + y(3\mathrm{Ni} + \mathrm{Al}) \rightarrow \mathrm{TiC} + y\mathrm{Ni_3Al} \qquad (1)$$

where y ranged from 25, 30, 40, 60 to 80 wt.%. First, the powders were mixed by dry milling with steel balls for 2 h and the blends were pressed into compacted samples. The length if the compact was 65 mm, the width was 10 mm and the thickness was 10 mm, operated at a pressure of 8 MPa to obtain the densities of 50% theoretical density. A small hole was drilled in the bottom of the compact, and a thermocouple pair (W–5%Re/W–26%Re) was inserted into the hole and linked to an X–Y recorder. The compacts were ignited at one end by laser irradiation using 5 kW CO_2 laser (HJ-4) with a fixed wavelength of 10.6 μm. The laser processing parameters in this study are selected as follows: laser power 1.2 kW, rectangular laser beam 10 mm × 10 mm.

The samples obtained were sawn and polished with SiC papers. The density of the sample was measured by the Archimedes law with water medium. To guarantee the accuracy of the real densities, each sample was measured five times and the final density data were obtained by averaging the five measurements. Therefore, except for the influence of the finest surficial open pores, the data accuracy is accepted. The microstructure and phase analysis of the composite of SHS were investigated by using field emission scanning electron microscopy (FESEM) (Model JSM-6700, Japan) equipped with energy-dispersive spectrum and XRD (Model D, Max2500PC, Rigaku, Japan).

3. Results and discussion

3.1. Reaction temperature

Fig. 2 shows the influence of y-value on ignition temperature (T_{ig}) and combustion temperature (T_c). From Fig. 2, it can be seen that ignition temperature (T_{ig}) hardly varies with increasing y-value, which indicates that the ignition temperature has nothing to do with the chemical composition of the system. It is worth noting that combustion temperature, T_c, decreases almost linearly with y-value increasing. This is attributed to the decrease of the heat generated of system with increasing y-value because enthalpy of formation of intermetallic compound Ni_3Al (−37.5 kJ/mol) is smaller than that of TiC (−184 kJ/mol), therefore, combustion temperature of system decreases. But the experimental measurements of T_c are lower than the corresponding T_{ad}, the reason for the discrepancy between the measured T_c and T_{ad} can be explained as follows: (1) the combustion temperature measured by the thermocouple may be lower than the actual combustion temperature in the specimen, because the combustion reaction rate is very fast and the combustion temperature gradient is very high during SHS while the response rate of the thermocouple is limited; (2) the SHS process cannot be ideally adiabatic, thus heat loss due to heat flow from the reaction zone to the surroundings is unavoidable, and the combustion temperature is lower than the adiabatic combustion temperature; (3) the reaction of $Ti_{(s)} + C_{(s)} \rightarrow TiC_{(s)}$ is uncompleted.

3.2. Density analysis

The sintered density, green density and porosity after sintering with different y-value are given in Figs. 3 and 4. From Fig. 3, it can be seen that sintered density is smaller than green density. This may be because there are large amounts of porosities in the sintered samples (as shown in Fig. 4). This porosity is due to the differences in specific volume between product and reactants, the evaporation of impurities, and the expansion of the

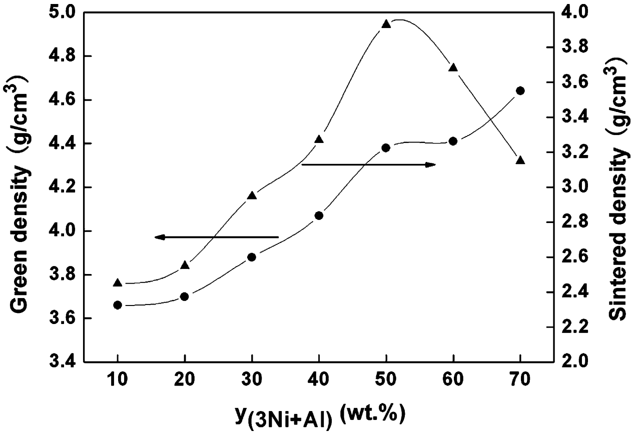

Fig. 3. Green density and sintered density related to *y*-value.

gas trapped in the porosity of the reactant compact. Furthermore, Fig. 3 also shows that sintered density increases before 50 wt.% *y*-value and then decreases with further increasing *y*-value. The maximum value of the sintered density is up to 3.93 g/cm^3 when *y*-value is 50 wt.%. The reason may be as follows: let us assume Ni_3Al is a filling phase, unconsidering the effect of sintering, the increase of *y*-value induces that more filling phase will fill in porosity, which increases density of products, porosity is occupied completely just as *y*-value is 50 wt.% (as shown in Fig. 5), therefore, density of products will emerge the maximum value when *y*-value is 50 wt.%. The reason for the decrease in sintered density for value of y higher than 50% may be the lower content of liquid phase formed as a consequence of the decrease in combustion temperature.

3.3. XRD results

Fig. 6 shows XRD patterns of TiC/Ni_3Al composites synthesized by the LISHS reaction with different *y*-value. It can be seen that TiC, Ni_3Al, Ni and Ti phases are detected in the reacted samples containing various *y*-value. This illuminates TiC and Ni_3Al are the two stable phases by laser ignited self-propagating high-temperature synthesis in Ti–C–3Ni–Al system. Furthermore, it also can be seen that relative intensity of TiC peaks and Ni_3Al peaks varies with different *y*-value. As the amount of *y*-value increases, the intensity of Ni_3Al peak is observed to increases and that of TiC peak decreases, especially, at Fig. 6(f), the Ni_3Al(1 1 0) peak can clearly be seen, and then it appears to diminish as the amount of *y*-value decreases, this indicates that the increasing of *y*-value causes less Ti to react with the C to form TiC.

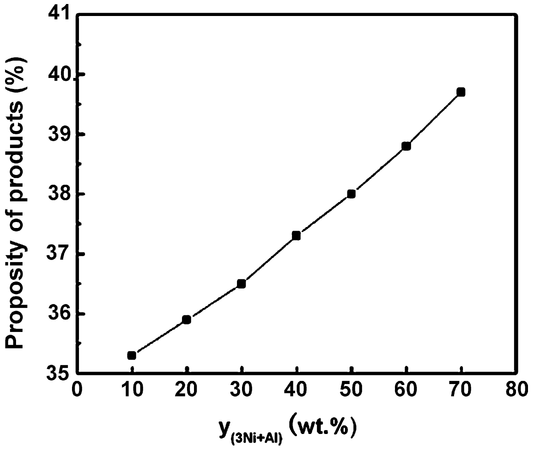

Fig. 4. Porosity of product related to *y*-value.

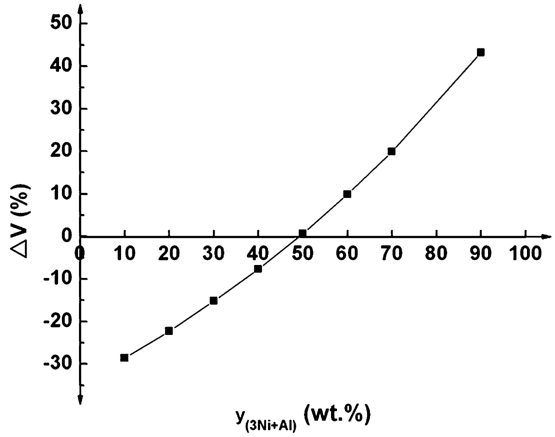

Fig. 5. Effect of plot of *V* on *y*-value. *V* = (3Ni + Al) content (vol.%)–product porosity (%).

To reflect a clearer comparison, the percentage of synthetic products in the master alloys synthesized by the starting materials with different *y*-value are roughly estimated based on the intensity of Ni(2 2 2), Ti(2 2 2), TiC(2 0 0) and Ni_3Al(1 1 1) diffraction peaks by the following equation:

$$x_i = \frac{1}{(K_i/I_i)\sum_{i=1}^{n}(I_i/K_i)} \tag{2}$$

where x_i, K_i and I_i are the percentage of synthetic products, reference intensity and diffracted intensity, respectively. The results are shown in Table 1. From Table 1, it can be seen that x_{TiC} and $x_{\mathrm{Ni_3Al}}$ with *y*-value = 25% were calculated to be 82.6 and 5.7%, respectively. When *y*-value is raised to 80 wt.%, x_{TiC}

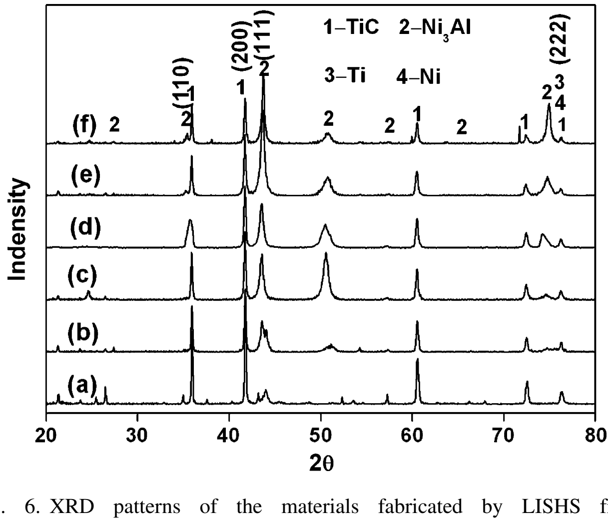

Fig. 6. XRD patterns of the materials fabricated by LISHS from (a) 75%(Ti + C) + 25%(3Ni–Al); (b) 70%(Ti + C) + 30%(3Ni–Al); (c) 60%(Ti + C) + 40%(3Ni–Al); (d) 50%(Ti + C) + 50%(3Ni–Al); (e) 40%(Ti + C) + 60%(3Ni–Al); (f) 20%(Ti + C) + 80%(3Ni–Al).

Table 1
Effect of *y*-value on the percentage of synthetic products of TiC, Ni_3Al, Ti and Ni roughly estimated based on the intensity of Ni(2 2 2), Ti(2 2 2), TiC(2 0 0) and Ni_3Al(1 1 1) diffraction peaks

y-Value in starting materials (wt.%)	The percentage of synthetic products			
	TiC	Ni_3Al	Ni	Ti
25	82.6	5.7	5.4	6.3
30	74.8	15.1	4.7	5.4
40	63.1	26.7	4.7	5.5
50	56.8	35.7	4.3	3.2
60	49.5	43.6	3.2	3.7
80	45.2	43.9	3.7	4.2

decreases to 45.2% while x_{Ni_3Al} increases to 43.9%. This indicates that the amount of TiC synthesized decrease and that of Ni_3Al synthesized increase with the increasing of *y*-value.

To further develop an understanding of the LISHS reaction in Ti–C–3Ni–Al system, the standard Gibbs free energy of the system has to be taken into consideration. According to the XRD results, Ni_3Al, TiC, Ni and Ti phases are detected as expected in the products. As a result, it can be proposed that the following reactions may take place in the Ti–C–3Ni–Al system [16]:

$$3Ni_{(s)} + Al_{(s)} \rightarrow Ni_3Al_{(s)} \quad \Delta G_1^0 = -175700 + 32.20T \tag{3}$$

$$Ti_{(s)} + C_{(s)} \rightarrow TiC_{(s)} \quad \Delta G_2^0 = -184800 + 12.55T \tag{4}$$

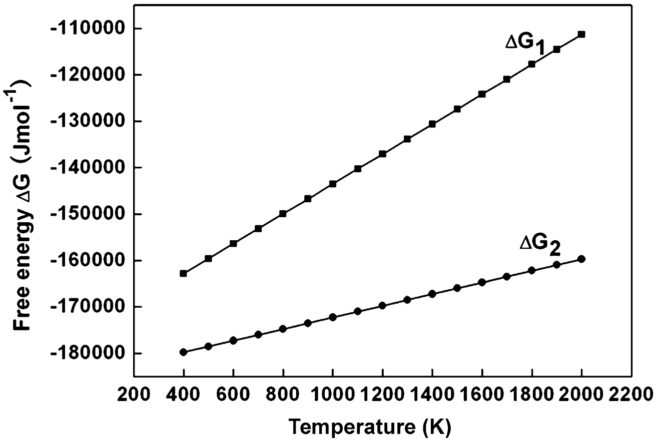

Fig. 7. Change of standard Gibbs free energy as a temperature for ΔG_1 and ΔG_2.

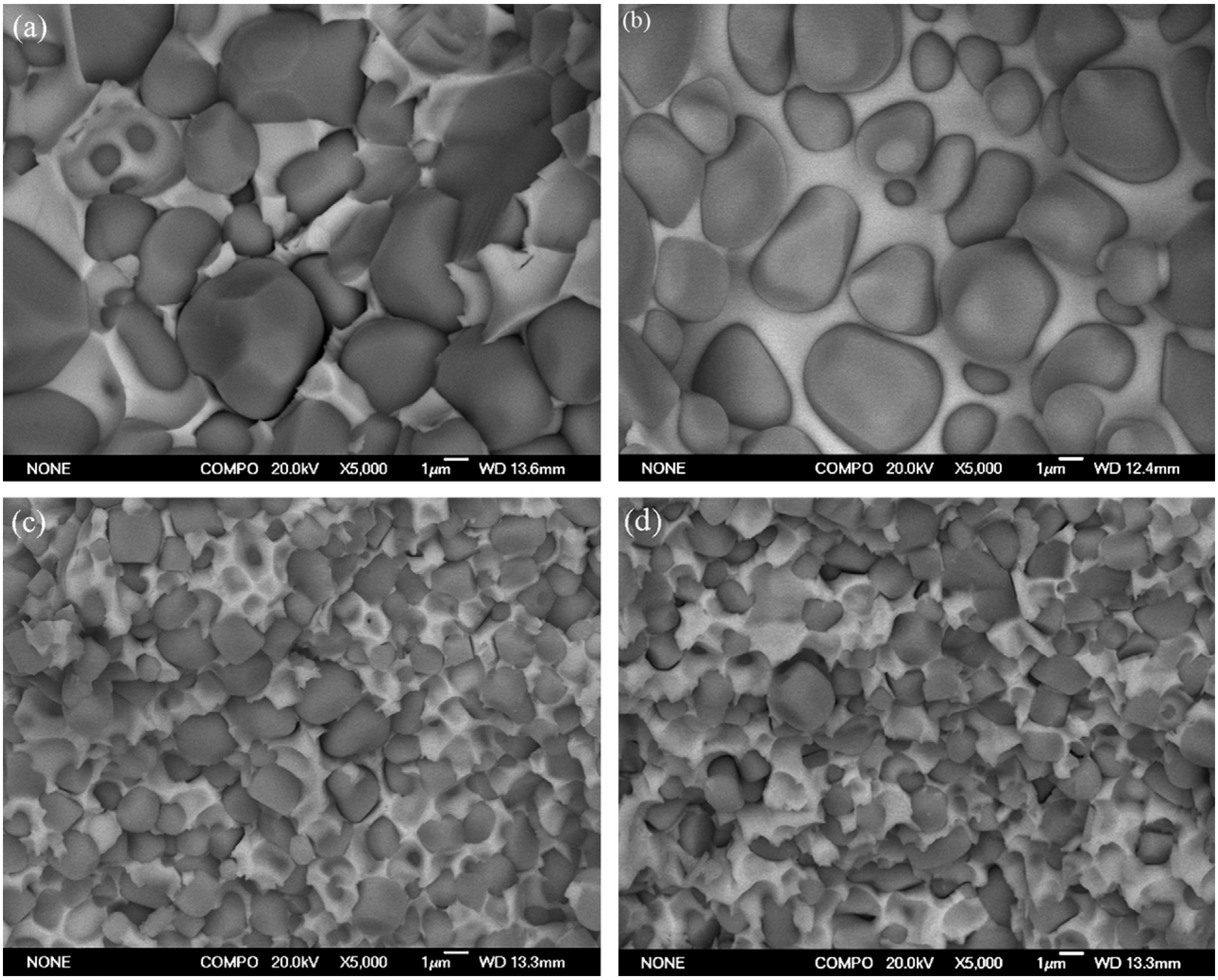

Fig. 8. Typical backscattered-electron micrographs of samples by LISHS reactions of Ti–C–3Ni–Al system with a laser power = 1200 W using different *y*-value: (a) 30 wt.%; (b) 50 wt.%; (c) 60 wt.%; (d) 80 wt.%.

To evaluate the possibility of these reactions, the standard Gibbs free energy change has been calculated and is shown in Fig. 7 as a function of temperature. It can be observed that the changes in standard Gibbs free energy of two reactions are all negative, which indicates that the above reactions are all favorable. It is worth noting that ΔG_2^0 is more negative for the formation of TiC in the temperature range of interest, and thus reaction (4) has a higher tendency for the formation of TiC than the reaction (3). Therefore, it can be deduced that the final equilibrium phases should consist of TiC. However, over the melting point of aluminum, the reaction for Ni_3Al formation is more favorable, kinetically, and hence occurs initially. The heat generated by the formation of the Ni_3Al phase may subsequently initiate the reaction of $Ti + C \rightarrow TiC$. Thus Ni_3Al as equilibrium phases is found in the final products. This results is in agreement with X-ray result, indicating that the phase constitution of the composites consists of Ni_3Al, TiC, Ni and Ti (see Fig. 6).

3.4. SEM analysis

Fig. 8 shows the typical backscattered-electron micrographs of the samples by SHS of Ti–C–3Ni–Al system with different *y*-value, because atomic number of Ni is bigger than that of Ti, it can be deduced that bright areas are Ni-rich zone, and greyer ones are Ti-rich zone. According to XRD patterns, the products synthesized consist of TiC, Ni_3Al, Ni and Ti, as shown in Fig. 6, in view of these results, it can be further confirmed that the bright areas are Ni_3Al phase of Ni-rich, the greyer ones are TiC phase of Ti-rich. Furthermore, TiC phase of Ti-rich is surrounded by Ni_3Al phase of Ni-rich in the infiltration zone. This may be reason that combustion temperature (T_c) is over melting point of Ni_3Al (1340 °C), as a results, Ni_3Al phase keeps molten state during combustion process (as shown in Fig. 2). From Fig. 8, we can also be seen that Ni-rich zone gradually increases and Ti-rich zone gradually decreases with the increasing of *y*-value, i.e., the content of Ni_3Al phase increases and that of TiC phase decreases.

As shown in Fig. 8, it can also be seen that the grain size of TiC synthesized decreases when *y*-value increases. This is attributed to the decrease of the combustion temperature (as shown in Fig. 2) because grain grown of TiC is an exponential function of the combustion temperature [17]. In addition, molten Ni_3Al phase serves as a diluent and might prevent the diffusion of Ti and C during the SHS reaction, which restrains the TiC crystals from further growth. However, it is be seen that the decreasing of grain size is unobvious when *y*-value is over 60 wt.%. We do not know why TiC grain size is not clear at higher Ni_3Al content ($y > 60$ wt.%). It may be because higher Ni_3Al content is beneficial from the growth of TiC, which compensates the effect of the decreasing of combustion temperature on TiC grain size, leading to the unobvious variety of TiC grain size at higher Ni_3Al content. That will be our tast in our further study.

4. Conclusions

TiC/Ni3Al composites have been successfully prepared by LISHS reaction of Ni, Al, C and Ti powders. The results show that *y*-value has a significant effect on combustion temperature, phase composition, the density of the products and the grain size of TiC. When *y*-value increases, combustion temperature, the grain size of TiC and the amount of TiC synthesized decrease and the density of the products increases and then decreases, a maximum value of density appears at 50 wt.% *y*-value. Furthermore, it can be seen that ignition temperature and the microstructural morphology of the products are hardly dependent on the *y*-value.

References

[1] A.G. Merzhanov, et al., Self-propagating high-temperature synthesis of inorganic compound, Dodklady Akademy Nauk USSR 204 (2) (1972) 429–432.
[2] A.G. Merzhanov, et al., in: Z.A. Munir, J.B. Holt (Eds.), Self-Propagating High-Temperature Synthesis: Twenty Years of Search and Finding in Combustion and Plasma Synthesis of High-Temperature Materials, VCH, New York, 1990, pp. 1–53.
[3] Z.A. Munir, et al., Self-propagating exothermicreac tions: the synthesis of high temperature materials by combustion, Mater. Sci. R. 3 (1989) 227–365.
[4] J.B. Holt, S.D. Dunmead, Self-heating synthesis of materials, Annu. Rev. Mater. Sci. 21 (1991) 305–334.
[5] D.P. Pope, S.S. Ezz, Mechanical properties of Ni3Al and nickel-base alloys with high volume fraction of gamma prime, Int. Mater. Rev. 29 (1984) 136–167.
[6] N.S. Stoloff, Physical and mechanical metallurgy of Ni3Al and its alloys, Int. Mater. Rev. 34 (1989) 153–183.
[7] M. Yamaguchi, Y. Umakoshi, The deformation behaviour of intermetallic superlattice compounds, Prog. Mater. Sci. 34 (1990) 1–148.
[8] T. Suzuki, Y. Mishima, S. Miura, γ solvus surface in Ni–Al–X (X: Cr, Mo, and W) ternary systems, ISIJ Int. 29 (1989) 78–84.
[9] A. Neckel, in: R. Freer (Ed.), The Physical and Chemistry of Carbides, Nitrides and Borides, Dordrecht, 1990, p. 458 pp.
[10] R.J. Meyer, E.H.E. Pietsch, Gmelins Handbooks of Inorganic Chemistry, vol. 41, 8th ed., Springer, Berlin, 1951, 357 pp.
[11] P. Ettymayer, W. Lengauer, in: R.B. King (Ed.), Encyclopedia of Inorganic Chemistry, Wiley, Chichester, 1994, 519 pp.
[12] L.M. Zhang, R. Tu, R.Z. Yuan, The TiC–Ni_3Al wettability and effect of Mo addition, J. Compos. Soc. (1995) (in China).
[13] B.C. Mei, J. Zhou, R.Z. Yuan, Kinetic of combustion synthesis in Ti–C–3Ni–Al system, Mater. Sci. Ed. 16 (2001) 1–5.
[14] J. Keskinen, J. Maunu, P. Lintula, M. Heinonen, P. Ruuskanen, TiC/Ni_3Al composites manufactured by self-propagating high-temperature synthesis and hot isostatic pressing, J. Mater. Synth. Process. 7 (1999) 253–258.
[15] L.M. Zhang, T. Hirai, A. Kumakawa, R.Z. Yuan, Cyclic thermal shock resistance of TiC/Ni3AI FGMs, Comp. B 28B (1997) 21–27.
[16] Y.J. Liang, Y.C. Che, Data Handbook of Mineral Thermodynamics, Northeastern Press, Shen Yang, 1993.
[17] Y. Choi, S.W. Thee, Effect of aluminium addition on the combustion reaction of titanium and carbon to form TiC, J. Mater. Sci. 8 (1993) 6669–6675.